arXiv:astro-ph/9812400v1 22 Dec 1998

Orbital evolution of a binary neutron star and gravitational radiation

Kuznetsov O.A.[1], Prokhorov M.E.[2],
Sazhin M.V.[2], Chechetkin V.M.[1]

[1] *Keldysh Institute of Applied Mathematics, Moscow*
kuznecov@spp.keldysh.ru; chech@int.keldysh.ru

[2] *Sternberg Astronomical Institute, Moscow*
mike@sai.msk.ru; sazhin@sai.msk.ru

Astronomy Reports, Vol.42, No.5, 1998, pp.638–648
Translated from Astronomicheskii Zhurnal
Vol.75, No.5, 1998, pp.725–735

Abstract—We consider the dependence of the internal structure of a neutron star in a close binary system on the semi-major axis of the binary orbit, focusing on the case when the Roche lobes of the components are nearly filled. We adopt a polytropic equation of state. The temporal evolution of the semi-major axis and its dependence on the mass ratio of the binary components and the polytropic index n are determined. The calculation are carried out right up to the moment of contact, when quasi-stationary model becomes invalid. We analyze differences in the shapes of the pulses of gravitational radiation emitted by a pair of point masses and by a binary neutron star, taking into account its internal structure and tidal deformations.

1 INTRODUCTION

Gravitational-wave astronomy is currently one of the most intensively developing branches of science. Coalescing neutron stars are especially interesting sources of gravitational radiation in the context of future gravitational-wave detectors. Binary neutron star exist in our Galaxy, and are observed as binary radio pulsars. Such systems lose energy via gravitational radiation; this causes the semi-major axis of the system orbit to decrease, ultimately leading to the coalescence (merging) of the stars. A large number of such systems for which the merging time is much less than the cosmological time are known, so that neutron stars merges should occur fairly often (no more rarely than about 3 events per year within a distance of 200 Mpc) [1–4]. Already operating and planned laser gravitational-wave detectors [3, 5, 6] will search for such events.

The merging process can be divided into three physically distinct stages.

1. The binary components move in quasi–Keplerian orbits without mass transfer, approaching each other only due to the emission of gravitational radiation.
2. Upon the stars become sufficiently close, mass transfer between the binary components must be taken into account in addition to the Keplerian motion and gravitational radiation.
3. In a late stage of the mass transfer, the merging of the binary components or falling of on star onto the other leads to the formation of a single object. This is the third stage of merging process. (Note that the distinction between the second and the third stages is quite arbitrary.)

This problem has been treated in a large number of studies, among which two different approaches can be distinguished. The first approach is analytical. It is useful for studies of very distant pairs, in which distortions in the shape of the stars due to their mutual gravitational attraction and other tidal effects are negligible. In this case, the problem can be reduced to a form that permits finite, analytical solution. A number of such studies account for post–Newtonian gravitational effects [7–9]. This approach fails for even moderately close pairs, in which tidal effects, rotation, and the internal structure of the components become substantial, and must be taken into account when deriving information from the gravitational-wave pulses emitted [10].

The second approach relies on numerical computations. It uses hydrodynamic codes to describe the non-stationary coalescing and merging of two bodies, taking into account a whole series of physical processes that may be important. This approach is the only able to describe the late stages of a merger [11]. Unfortunately, current hydrodynamic codes have a number of drawbacks, including the presence of artificial viscosity in the numerical algorithms used and the inability to follow the evolution of a binary system from large values of the semi-major axis (say, $\sim 10^6$ stellar radii) up to contact.

The first (analytical) method is able to trace the binary evolution up to a hundred stellar radii rather accurately, while the second (hydrodynamical) method can be used to calculate the evolution of the system beginning from several stellar radii. Thus, there remains an appreciable interval of semi-major axis values (say, from 100 to 5–10 $R_\star$) for which different methods must be applied. We describe below one possible method in which quasi-stationary stellar configurations are calculated fully taking into account tidal effects.

We will focus on a detailed description of the first stage, when the stars move only under the action of their mutual gravitational attraction and gravitational radiation. The problem will be solved numerically using the code developed in [12]. The second part of the problem is the determination of the shapes of gravitational-wave pulses emitted and identification of characteristic features that can be used to derive the main parameters of neutron stars.

2 A MODEL FOR AN EQUILIBRIUM POLYTROPIC STAR IN A BINARY SYSTEM

We consider a model for a binary star with component masses M_1 and M_2 and total mass $M = M_1 + M_2$. We assume the orbit to be circular with radius A; this assumption should be reasonable, since the orbit should be circularize long before the final stage of coalescence due to emission of gravitational radiation [7]. The primary component is treated as a polytropic star with polytropic index n, while the secondary is taken to be a point mass. Below, we will present arguments showing that this assumption is justified. As in [12], we chose the coordinate origin to be at the center of the first component, and the orthogonal coordinate axes to be oriented so that Ox passes through the centers of the two stars and Oy lies in the orbital plane.

The equation of state of the first star is

$$P = K\rho^{1+1/n}$$

where P and ρ are the pressure and density of the stellar matter and K is the polytropic constant. The density and the potential distributions are described by the equation of hydrostatic equilibrium:

$$\Phi_1 + \Phi_2 + \Phi_c + K(n+1)\rho^{1/n} = B\,, \tag{1}$$

where Φ_1 is the potential of the first star (both inside and outside), Φ_2 is the potential of the second star (point mass)

$$\Phi_2 = -\frac{GM_2}{\sqrt{(x-A)^2 + y^2 + z^2}}\,,$$

Φ_c is the centrifugal potential, and B is a constant determined by the boundary conditions. The centrifugal potential is taken in the form

$$\Phi_c = -{}^1\!/_2\Omega^2[(x - X_c)^2 + y^2]\,,$$

where X_c is the center of mass of the system. In contrast to [12], we do not use the Keplerian formula for the semi-major axis for a given angular velocity Ω. Instead, we determine this value self-consistently, taking into account the tidal interaction of the stars:

$$\frac{\partial}{\partial x}\,(\Phi_1 + \Phi_c)|_{(A,0,0)} = 0\,.$$

On the other hand, the density and potential of the first star are related by the Poisson equation

$$\Delta\Phi_1 = 4\pi G\rho\,. \tag{2}$$

To find the equilibrium configuration for the extended component of the system, we must solve the system of equation (1) and (2) using the condition

$$\int \rho_1 dV_1 = M_1\,.$$

To implement the numerical algorithm, it is convenient to use the following dimensionless variables. We will express distances in units $L = (GM/\Omega^2)^{1/3}$, masses in units of M_2, densities in units of M_2/L^3, the gravitational potential in units of GM_2/L, and the polytropic constant in units of $GM_2^{1-1/n}L^{3/n-1}$. As a result, we arrive at the dimensionless equations

$$\phi_1 + \phi_2 + \phi_c + \kappa(n+1)\rho^{1/n} = b\,, \tag{3}$$

$$\Delta\phi_1 = 4\pi\rho\,, \tag{4}$$

$$\int \rho dV = q\,, \qquad q = M_2/M_1\,, \tag{5}$$

$$a = A/L\,, \tag{6}$$

$$\phi_2 = -\frac{1}{\sqrt{(x-a)^2 + y^2 + z^2}}\,, \tag{7}$$

$$x_c = q^{-1}\int x\rho dV = 0\,, \tag{8}$$

$$\phi_c = -\,{}^1\!/_2(q+1)\left(\left(x - \frac{a}{1+q}\right)^2 + y^2\right)\,, \tag{9}$$

$$\frac{\partial}{\partial x}\,(\phi_1 + \phi_c)|_{(a,0,0)} = 0\,, \tag{10}$$

$$\phi_1 \to -q/\sqrt{x^2+y^2+z^2}\,, \qquad x,y,z \to \infty \tag{11}$$

in which lower-case letters denote dimensionless variables, κ is the dimensionless polytropic constant, and ρ is now the dimensionless density.

3 NUMERICAL ALGORITHM

We transformed the system of equations to dimensionless form and solved it using the iterative method described in detail in [12]. We will now briefly summarize this method.

Let M_1, M_2, Ω K, and n, be given, while A, B, $\rho(x,y,z)$, and $\Phi_1(x,y,z)$ must be determined. We do not assume *a priori* that Kepler's third law $A^3\Omega^2 = GM$ is satisfied. In dimensionless form, the input parameters are q, κ, and n (note that $m_2 = 1$, $m_1 = q$, and $\omega = \sqrt{q+1}$ in dimensionless form), while a, b, $\rho(x,y,z)$, and $\phi_1(x,y,z)$ must be found. The dimensionless form of Kepler's third law is $a = 1$. All calculations were performed for the case $q = 1$ and $n = {}^3/_2$, and κ was varied. This is in accordance with the relation $K = \kappa G M_2^{1-1/n} L^{3/n-1}$, which is equivalent to the shrinking of the system with fixed polytropic constant K, with $\kappa \to 0$ corresponding to an infinitely wide system ($L \to \infty$).

The calculations can be applied to systems with any M_1 and K. However, to make the results more transparent, we will scale them to correspond to a binary system in which $M_1 = M_2 = 1.4M_\odot$ and the radius of unperturbed neutron star is 10 km. In this case of an infinitely wide pair, when the first component is purely spherical, this corresponds to an average density for the first component $\bar{\rho}_1 = 6.68 \times 10^{14}\mathrm{g/sm}^3$ and a polytropic constant $K = 3.99 \times 10^9 \mathrm{cm}^4\mathrm{g}^{-2/3}\mathrm{s}^{-2}$.

The scheme for the solution of the system of equation (3)–(11) is, in many ways, analogous to that in [12], with the addition of two more iteration cycles to solve the equations $x_c = 0$ and (10). These differences from [12] are associated with the necessity of determining a, which, in general, differs from unity (i.e. Kepler's third law is not necessarily valid for a distributed mass). We note, however, that the value for a returned by the computer code deviates from the unity by less then 0.5%.

4 GRAVITATIONAL RADIATION FROM A BINARY SYSTEM WITH AN EXTENDED COMPONENT

Energy losses due to emission of gravitational waves are described by the formula [13]

$$-\frac{\partial E}{\partial t} = \frac{G}{45c^5} \overset{\bullet\bullet\bullet}{Q}{}^2_{\alpha\beta} \,, \tag{12}$$

where

$$Q_{\alpha\beta} = \int \rho \left(x_\alpha x_\beta - {}^1\!/_3 \delta_{\alpha\beta} x^2 \right) dV$$

Since the rate of change of the orbit at the end of its evolution is comparable to the velocities of the components, we must, in general, take into account the first and higher time derivatives of the semi-major axis.

The main formulas for our analysis are presented for a rotating coordinate system. For transformation of quantities to a non-rotating frame, we write expressions for quadrupole moments of the system and of individual bodies in non-rotating and rotating coordinate systems. We denote the non-rotating frame by $O\hat{x}\hat{y}\hat{z}$, and add a sign ˆ over all quantities related to this frame. We keep the notation $Oxyz$ for the rotating frame, and quantities in this frame will be presented without a sign ˆ. The transformations from the rotating to the non-rotating coordinate system are given by equations

$$x = \hat{x} \cos\psi(t) - \hat{y} \sin\psi(t) \,,$$

$$y = \hat{x} \sin\psi(t) + \hat{y} \cos\psi(t) \,,$$

where $\overset{\bullet}{\psi}(t) \equiv \Omega(t)$ is the time-dependent angular velocity of the binary system.

Recall that our model for the binary system consists of a primary component that is a polytropic star under hydrostatic equilibrium in the rotating frame and a secondary component that is a point mass. The quadrupole tensor of such a binary system in the rotating frame can be written as

$$Q_{\alpha\beta} = m_1 (r_{1\alpha} r_{1\beta} - {}^1\!/_3 \delta_{\alpha\beta} r_1^2) + m_2 (r_{2\alpha} r_{2\beta} - {}^1\!/_3 \delta_{\alpha\beta} r_2^2) + q_{\alpha\beta} \,,$$

where we have introduced the notation

$$q_{\alpha\beta} = \int d^3\xi \rho_1(\xi) (\xi_\alpha \xi_\beta - {}^1\!/_3 \delta_{\alpha\beta} \xi^2)$$

for the quadrupole tensor of the distributed mass, while the first and second terms are the contributions to the quadrupole tensor of two point masses located at $\boldsymbol{r} = \boldsymbol{r}_1$ and $\boldsymbol{r} = \boldsymbol{r}_2$ respectively. Here, ξ are the coordinates relative to the center of mass of the first star $\boldsymbol{r} = \boldsymbol{r}_1$.

It is known [13] that the quadrupole tensor can be expressed in terms of the inertia tensor of the first star

$$I_{\alpha\beta} = \int d^3\xi \rho_1(\xi) (\delta_{\alpha\beta} \xi^2 - \xi_\alpha \xi_\beta)$$

in accordance with the expressions

$$q_{\alpha\beta} = {}^{1}\!/_{3}\delta_{\alpha\beta} I - I_{\alpha\beta}\,,$$

where $I = I_{XX} + I_{YY} + I_{ZZ}$ is the trace of the inertia tensor.

Since $\boldsymbol{r}$ is defined for the baricenter of the system, we can find explicit expressions for the vectors of each component in the form

$$\boldsymbol{r}_1 = \frac{m_2 A}{m_1 + m_2}(1,\ 0,\ 0)\,,$$

$$\boldsymbol{r}_2 = \frac{m_1 A}{m_1 + m_2}(-1,\ 0,\ 0)\,.$$

Now, the explicit form of the quadrupole tensor in the rotating frame will be a function of two parameters: the quadrupole tensor of the system of point masses, which is determined by μA^2 (μ is the reduced mass of the binary system), and the quadrupole tensor of the extended component $q_{\alpha\beta}$. Since our model is symmetrical with respect to the planes $y = 0$ and $z = 0$, only three of nine components of the quadrupole tensor are non-zero: q_{XX}, q_{YY}, and q_{ZZ}. Since the trace is equal to zero ($q_{XX} + q_{YY} + q_{ZZ} = 0$), there remain only two independent parameters, which fully describe the total quadrupole tensor of the binary system in the rotating frame:

$$f_1 = \frac{\mu A^2}{6} + \frac{q_{XX} + q_{YY}}{2}\,,$$

$$f_2 = \frac{\mu A^2}{2} + \frac{q_{XX} - q_{YY}}{2}\,.$$

We now write the components of the quadrupole tensor in the non-rotating frame:

$$\hat{Q}_{XX} = f_1 + f_2 \cos 2\psi(t)\,,$$

$$\hat{Q}_{XY} = -f_2 \sin 2\psi(t)\,,$$

$$\hat{Q}_{YY} = f_1 - f_2 \cos 2\psi(t)\,,$$

$$\hat{Q}_{ZZ} = -2f_1\,,$$

$$\hat{Q}_{XZ} = \hat{Q}_{YZ} = 0\,.$$

In the case of stationary orbit ($\dot{\Omega}= 0$), the formula for gravitational radiation differs from the standard formula of two point masses [13] only in a term of the form $q_{XX} - q_{YY}$:

$$-\frac{dE}{dt} = \frac{32G}{5c^5}\Omega^6(\mu A^2 + q_{XX} - q_{YY})^2$$

This formula reduces to the known relation [13]

$$-\frac{dE}{dt} = \frac{32G}{5c^5}\Omega^6(\mu A^2)^2 = \frac{32G}{5c^5}\Omega^6 A^4 \left(\frac{M_1 M_2}{M}\right)^2$$

in the case of point masses ($q_{XX} = q_{YY} = 0$). Given the density distribution in the extended component of the system, we can calculate the dimensionless quadrupole momentum of this component with respect to the center of mass. Let us introduce the dimensionless function

$$f = \frac{q}{1+q}\left[\left(\frac{A}{L}\right)^2 - 1\right] + \frac{q_{XX} - q_{YY}}{M_2 L^2}$$

so that the luminosity of the binary system in the form of gravitational waves is

$$-\frac{dE}{dt} = \frac{32G^4 M_2^5}{5c^5 L^5}\left(\frac{q}{1+q} + f\right)^2 (1+q)^3$$

Using the relation $K = \kappa G M_2^{1-1/n} L^{3/n-1}$, we eliminate L and obtain

$$-\frac{dE}{dt} = \frac{32G^{\frac{12+n}{3-n}} M_2^{\frac{10}{3-n}}}{5c^5 K^{\frac{5n}{3-n}}}\kappa^{\frac{5n}{3-n}}\left(\frac{q}{1+q} + f(\kappa)\right)^2 (1+q)^3$$

Note that, in the case of binary systems in which extended components are elongated along the line through the stellar centers, taking into account the proper moment of inertia of a component will always lead to an increased energy-loss rate compared to the case of point masses.

5 TOTAL ENERGY OF THE SYSTEM IN A MODEL WITH AN EXTENDED COMPONENT

If the energy loss $\dot{E}$ is known, we can calculate the shrinking velocity of the stars $\dot{E}= dE/dA \cdot \dot{A}$. In the standard approach [13], the energy of the system is taken to be the sum of gravitational energy of two point passes E_{12} and their kinetic energies K_1 and K_2. This yields an expression for the energy of the system $E = -GM_1M_2/2A$. If the masses are not point-like, we must also take into account the self-gravitational energies E_1^{self} and E_2^{self}, the internal energies E_1^{int} and E_2^{int}, and the kinetic energies of rotation of the stars about their centers of mass K_1^* and K_2^*. We will take the second component to be point so that $E_2^{self} = E_2^{int} = K_2^* = 0$. Then

$$E = E_{12} + K_1 + K_2 + E_1^{self} + E_1^{int} + K_1^* \,,$$

$$E_{12} = \int \rho \Phi_2 dV_1 \,, \qquad E_1^{self} = {}^1\!/_2 \int \rho \Phi_1 dV_1 \,,$$

$$K_1 = {}^1\!/_2 \Omega^2 M_1 \left(\frac{M_2}{M} A \right)^2 \,, \qquad K_2 = {}^1\!/_2 \Omega^2 M_2 \left(\frac{M_1}{M} A \right)^2 \,,$$

$$K_1^* = {}^1\!/_2 \Omega^2 I_{ZZ} \,, \qquad E_1^{int} = n \int P dV_1 = nK \int \rho^{1+1/n} dV_1 \,.$$

Let us now consider the asymptotic of E_1^{int}, E_1^{self} as $L \to \infty$. In this case, the first component can be considered a polytropic, self-gravitating sphere. The solution of the equilibrium equations for such configurations are well known [14,15]. The total energy of a polytropic, self-gravitating sphere in hydrostatic equilibrium is given by the formula [14,16]

$$E_1^{self} + E_1^{int} = -\frac{3-n}{5-n} \frac{G M_1^2}{R_1} \,.$$

The polytropic constant of such a sphere is determined by its mass and radius [14]:

$$K = \mathcal{N}_n G M_1^{\frac{n-1}{n}} R_1^{\frac{3-n}{n}} \,.$$

The coefficient $\mathcal{N}_n$ is associated with the solution of Lane-Emden equation[1] via the formula

$$\mathcal{N}_n = (4\pi)^{1/n} (n+1)^{-1} \xi_1^{-\frac{3-n}{n}} \mu_1^{-\frac{n-1}{n}} \,,$$

$$\mathcal{N}_{3/2} = 0.424 \,.$$

On the other hand,

---

[1] The Lane-Emden equation has the form

$$\xi^{-2} (\xi^2 \theta')' = -\theta^n \,,$$

where ξ is the independent variable and $\theta(\xi)$ is the desired function ($\theta' \equiv d\theta/d\xi$), with the boundary conditions given by

$$\theta(0) = 1 \,, \qquad \theta'(0) = 0 \,,$$

and by the values at the boundary of the sphere ξ_1: $\theta(\xi_1) = 0$, and $\mu_1 = -\xi_1^2 \theta'(\xi_1)$.

$$K = \kappa G M_2^{\frac{n-1}{n}} L^{\frac{3-n}{n}} \,.$$

We find as a result

$$E_1^{self} + E_1^{int} \to E_0 \left(-\frac{3-n}{5-n} \mathcal{N}_n^{\frac{n}{3-n}} q^{\frac{5-n}{3-n}} \right) = E_\infty \,, \qquad L \to \infty \,,$$

$$E_0 = G^{\frac{3}{3-n}} M_2^{\frac{5-n}{3-n}} K^{-\frac{n}{3-n}} \,.$$

The sum of energies $E_{12} + K_1 + K_2$ has the following asymptotic as $L \to \infty$:

$$E_{12} + K_1 + K_2 = E_0 \left(-{}^1\!/_2 q \kappa^{\frac{n}{3-n}} \right) \,.$$

We finally obtain for the total energy of the system the formula

$$E = E_0 \left(-{}^1\!/_2 q \kappa^{\frac{n}{3-n}} + h(\kappa) \right) + E_\infty \,.$$

Here, $h(\kappa)$ is determined from calculations of this function (equal to the sum K_1^* and the differences of $E_1^{self} + E_1^{int}$ and $E_{12} + K_1 + K_2$ from their limiting values), with $h(\kappa) \to 0$ as $\kappa \to 0$ (i.e., as $L \to \infty$):

$$h(\kappa) = \frac{E - E_0 \left(-{}^1\!/_2 q \kappa^{\frac{n}{3-n}} \right) - E_\infty}{E_0} \,.$$

Since the first component expands as the two components become closer, $h(\kappa) > 0$.

6 METRIC OF THE GRAVITATIONAL-RADIATION FIELD

The physical observed quantities in gravitational-wave astronomy are the transversely traceless corrections to the metric tensor h_+^{TT} and $h_\times^{TT}$. These are expressed in terms of time derivatives of the components of the quadrupole tensor of the system. To write the explicit form of the corrections to the metric tensor, we introduce a coordinate system that is rotated by the angle θ about the Oy axis. We will calculate the transversely traceless corrections to the metric along the $O\hat{x}$ axis in this new frame. The projection operator used to reduce the tensor to a transversely traceless for can be written

$$\hat{P} = \begin{pmatrix} 0 & 0 & 0 \\ 0 & 1 & 0 \\ 0 & 0 & 1 \end{pmatrix} \,.$$

We can now obtain the transversely traceless components of the quadrupole tensor in the new coordinate system:

$$Q_+^{TT} = {}^3\!/_2 f_1 \cos^2\theta - f_2 \frac{1+\sin^2\theta}{2} \cos 2\psi \,,$$

$$Q_\times^{TT} = f_2 \sin\theta \sin 2\psi \,.$$

The transversely traceless corrections to the metric are found using the time derivatives of the reduced components of the quadrupole tensor

$$h_+^{TT} = -\frac{2G}{3c^4 R_0} \overset{\bullet\bullet}{Q}{}_+^{TT}$$

$$h_\times^{TT} = -\frac{2G}{3c^4 R_0} \overset{\bullet\bullet}{Q}{}_\times^{TT}$$

where R_0 is the distance from the observer to the binary system.

7 EQUATION FOR THE CONVERGENCE OF THE COMPONENTS; CALCULATION RESULTS

The equation describing the convergence of a point mass and an extended component differs from that for two point masses. We will now determine how these equations change in our model and find the dependence of the main characteristics of the radiation on the parameters of the problem.

First, some introductory words are necessary. The semi-major axis of the system is denoted A, while the main calculations use the arguments L. We emphasize that the difference between L and A is small. Therefore, we will write all functions as arguments of L, and assume A and L to be identical. The geometrical properties if the system for various κ are depicted in Fig. 1, which shows the boundary of the star along the X-axis (asterisks) and the position of the point L_1. The horizontal and vertical axes plot X and L_1, both measured in terms of R_1. In addition, the values if dimensionless polytropic constant κ are marked on the axis to the right. We can see from Fig. 1 that the components are in contact if $\kappa = 0.153$, which is corresponds to $L/R_1 = 2.75$ (these estimates are independent of the chosen values of M_1 and K, and are entirely determined by q and n). In addition, we can see from Fig. 1 that the size of the first component is very insensitive to the location of the second component when $L/R_1 > 3.5$: $X_{min} = X_{max} = R_1$.

Since the resulting formulas are quite cumbersome, we will restrict the following discussion to the case $n = {}^3\!/_2$, $q = 1$, for which we performed our calculations. We then have

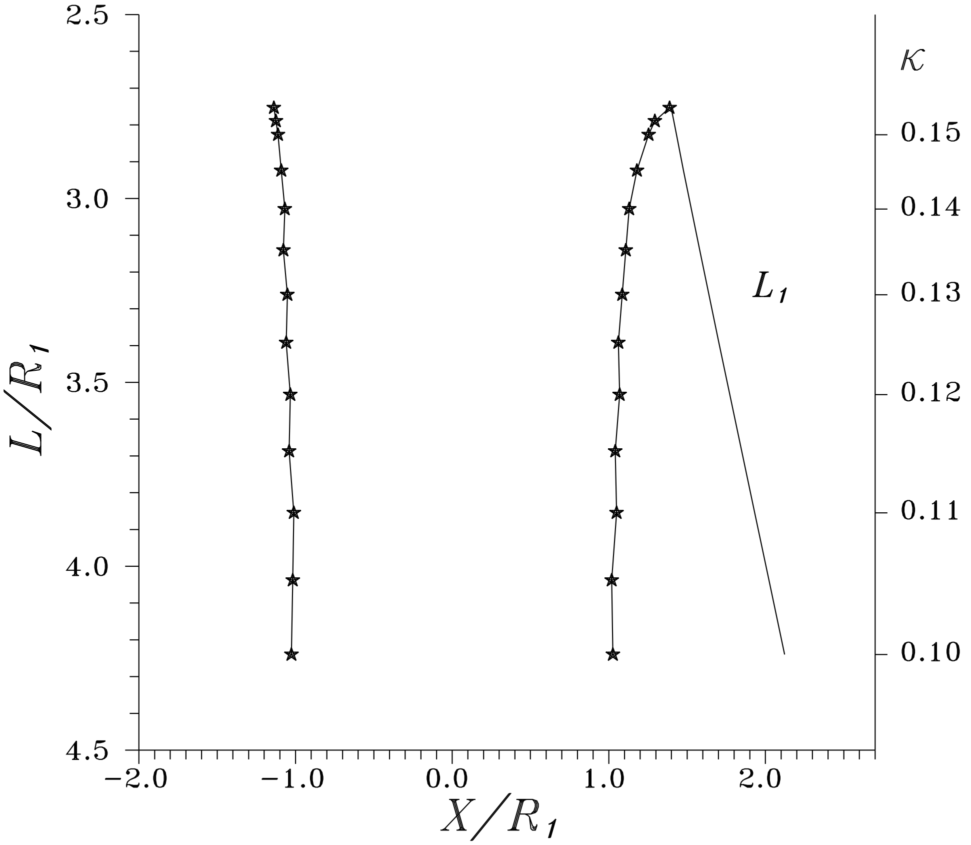

Figure 1: *Geometrical characteristic of the system. The Ox axis shows the boundary of the extended component: the left mark corresponds to the far side with respect to L_1, and the right mark to the near side. R_1 is the radius of the extended component for an infinitely distant point-mass component. The solid line shows the position of the Lagrange point L_1. The dimensionless polytropic constant κ is indicated on the supplementary vertical axis. The contact of the extended component with L_1 occurs at $L = 2.75R_1$.*

$$-\frac{dE}{dt} = \frac{256G^9M_2^{20/3}}{5c^5K^5}\kappa^5\left({}^1\!/_2 + f(\kappa)\right)^2 .$$

A plot of the function $f(\kappa)$ is given in Fig. 2, in which the solid line shows an approximation to this function using the formula $f(\kappa) = 171\kappa^{5.4}$. We then have for the total energy of the system

$$E = \frac{G^2M_2^{7/3}}{K}\left(-\frac{\kappa}{2} - {}^3\!/_7\mathcal{N}_{3/2} + h(\kappa)\right) .$$

The function $h(\kappa)$ was also calculated. This function can be approximated by the relation $h(\kappa) = 13.5\kappa^{4.1}$ (Fig. 3).

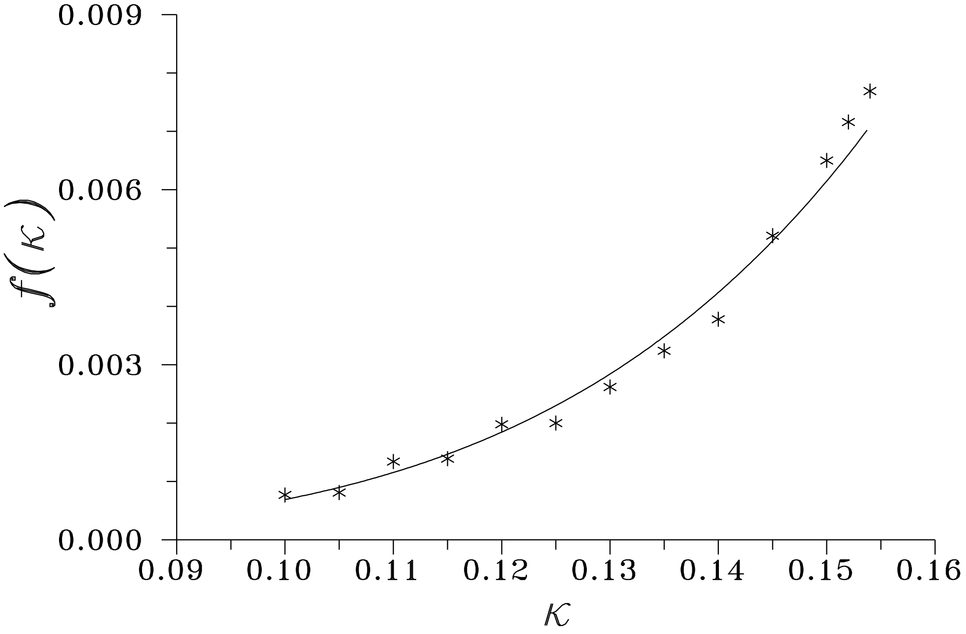

Figure 2: *Plot of the function* $f(\kappa)$ *showing how much the intensities of gravitational-wave radiation differ for extended-component and point-mass models. The solid line is the approximation* $f(\kappa) \approx 171\kappa^{5.4}$.

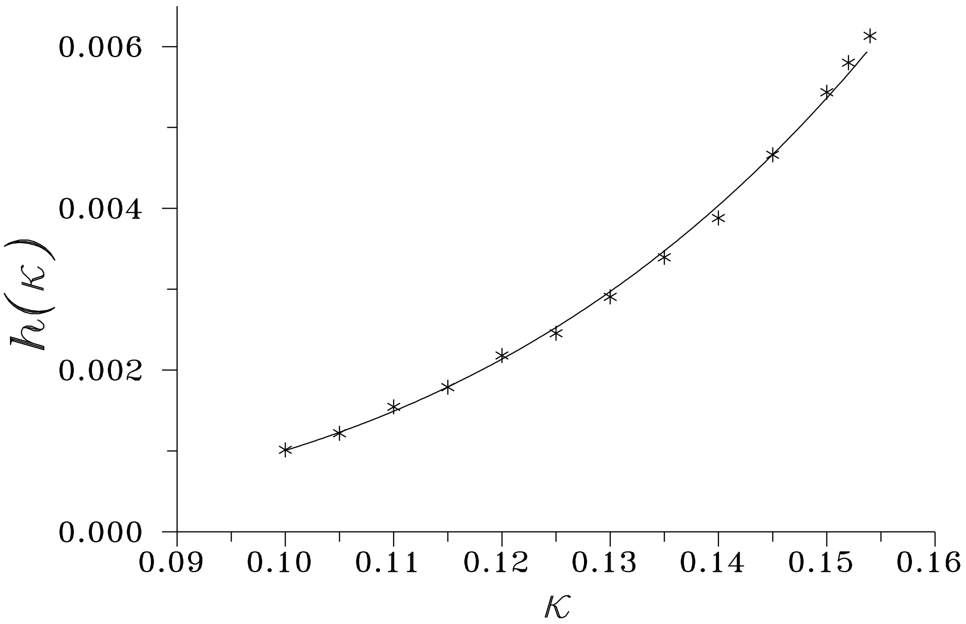

Figure 3: *Plot of the function* $h(\kappa)$ *showing how the total energy of a system with an extended component changes as to the total energy for two point masses. The solid line is the approximation* $h(\kappa) \approx 13.5\kappa^{4.1}$.

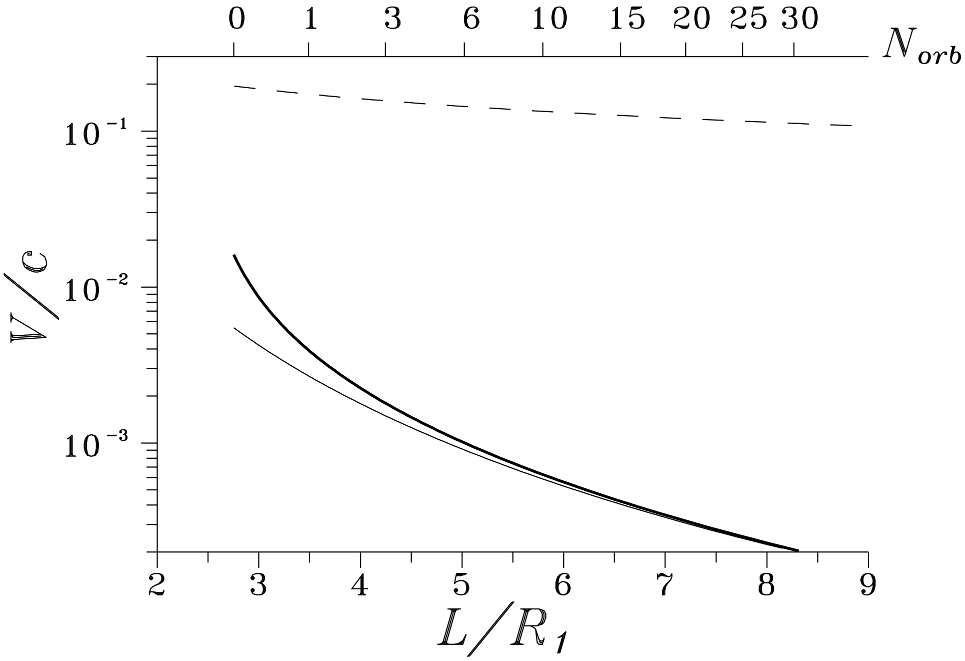

Figure 4: *Velocity of one of the component with respect to the center of mass of the system. The thick and thin lines correspond to the cases of extended and point masses, respectively. The dashed line shows the orbital velocity of the system* $^1/_2 A\Omega$.

We performed the calculations for a system consisting of one point mass and one extended component (this was associated with limitations of our computational capabilities, and this restriction will be relieved in the future). The results can be applied to two types of astrophysical objects:

- binary systems consisting of a black hole and neutron star of the same masses;
- binary systems consisting of two identical neutron stars.

The first case seems unrealistic because of evolutionary considerations, though there do exist models that predicts the formation of low-mass black holes in binaries [17].

We believe the second case to be more interesting. Using the above results, we can study such a system quite easily. Suppose the secondary component is also extended, and has the same configuration as the primary component, since their masses are equal. In this case the change associated with substituting the secondary point mass by an extended mass distribution is a correction of the next highest order, which can be neglected. It is necessary to double the corresponding terms in the formulas for the energy loss rate and the total energy of the system ($f(\kappa)$, $h(\kappa)$, and the term corresponding E_∞):

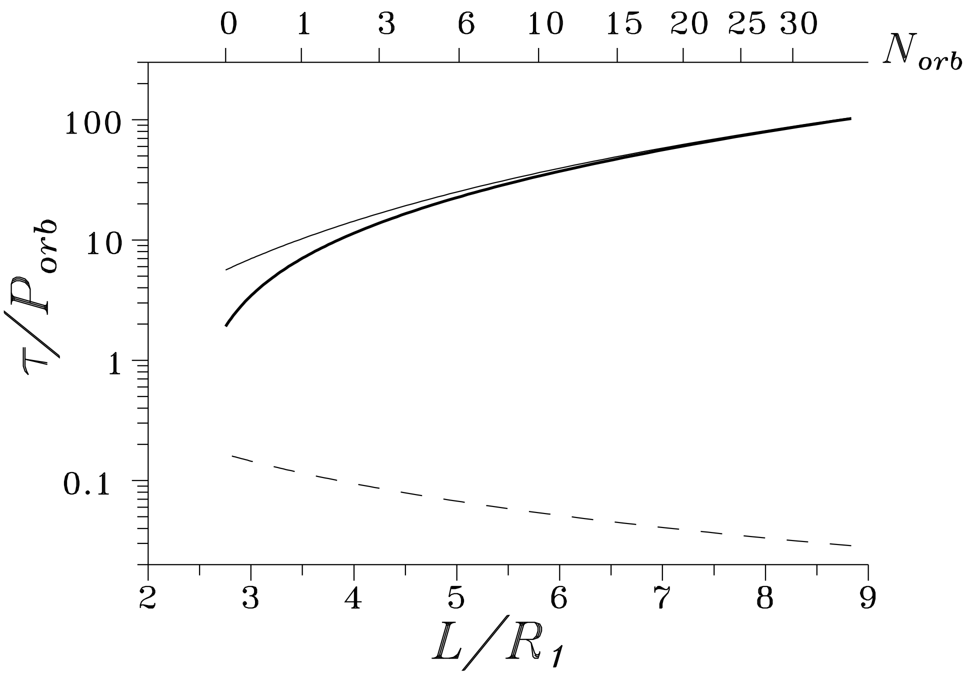

Figure 5: *Rate of radial shrinkage of the components* $\tau = L/\dot{L}$ *in units of the orbital period. The thick and thin lines correspond to the case of extended and point masses, respectively. The dashed line shows the characteristic hydrodynamic time for the extended component, which indicates how quickly equilibrium is reached inside the star. The number of orbital periods until contact is indicated on the upper axis.*

$$-\frac{dE}{dt} = \frac{256 G^9 M_2^{20/3}}{5 c^5 K^5} \kappa^5 \left({}^1\!/_2 + 2 f(\kappa)\right)^2 ,$$

$$E = \frac{G^2 M_2^{7/3}}{K} \left(-\frac{\kappa}{2} - 2\,{}^3\!/_7 \mathcal{N}_{3/2} + 2 h(\kappa) \right) .$$

Differentiating the second formula, we obtain

$$\frac{dE}{dt} = \frac{G^2 M_2^{7/3}}{K} \left(-{}^1\!/_2 + 2 h'(\kappa)\right) \frac{d\kappa}{dt}$$

and finally

$$\frac{d\kappa}{dt} = \frac{256 G^7 M_2^{13/3}}{5 c^5 K^4} \frac{\kappa^5 \left({}^1\!/_2 + 2 f(\kappa)\right)^2}{{}^1\!/_2 - 2 h'(\kappa)} .$$

Using the relations

$$\kappa = \frac{K}{G M_2^{1/3} L} ,$$

$$\frac{dL}{dt} = -\frac{GM_2^{1/3}L^2}{K}\frac{d\kappa}{dt}\,,$$

we can now obtain a differential equation for L:

$$-\frac{dL}{cdt} = {}^{16}\!/_5 \left(\frac{r_g}{L}\right)^3 \alpha(L)\,, \tag{13}$$

where $r_g = 2GM_2/c^2$, which is $r_g = 4.15$ km for the adopted value of M_2. The auxiliary quantity α is defined by the relation:

$$\alpha(L) = 1 + 15.5 \cdot \left(\frac{R_1}{L}\right)^{3.1} + 13.3 \cdot \left(\frac{R_1}{L}\right)^{5.4}\,, \tag{14}$$

where $R_1 = 10$ km is the radius of the unperturbed neutron star. Note that the maximum value $\alpha = 1.73$ is reached at the moment of contact of the components, when $L = 2.75R_1$. In the beginning of our calculations $L = 8.5R_1$, $\alpha = 1.02$. The accuracy of this formula is better than 1% (this maximum value is reached at the point of contact). It is not difficult to verify that our results returns the standard expression

$$\frac{dL}{dt} = -\frac{128G^3M_2^3}{5c^5L^3}$$

for a point-mass binary when $f(\kappa) = h'(\kappa) = 0$ and $\alpha = 1$.

Equation (13) describes the self-consistent evolution of a binary containing extended components due to emission of gravitational radiation. Our equations differ from those for a point-mass model in two new functions $f(L)$ and $h(L)$. Precisely these functions lead the differences in the evolution for these two models. The most important difference is the deviation of the function $\alpha(L)$ from unity in the model with extended components. This function is presented in a form convenient for comparison with post–Newtonian corrections to the law of motion for two point masses in a binary system.

The evolution of a binary system with extended components differs most from the evolution for two point masses in the final stages, when the effect of tidal distortions becomes significant. Therefore, below, we will compare two cases: a binary system consisting of two extended components and binary consisting of two point masses.

The next set of figures each show two lines: the thick line corresponds to the case of extended masses ant the thin line to the point-mass case. In addition, the number of orbital periods until contact is given on the upper axis on each plot.

Figure 4 presents the right-hand side if differential equation (13) in the form of convergence velocity of the components $V = {}^1\!/_2\,\overset{\bullet}{L}$ (in units of velocity of light c) as a function of the distance between the components. The characteristic orbital velocity of the system ${}^1\!/_2\Omega L$ is shown by the dashed line. Note that the

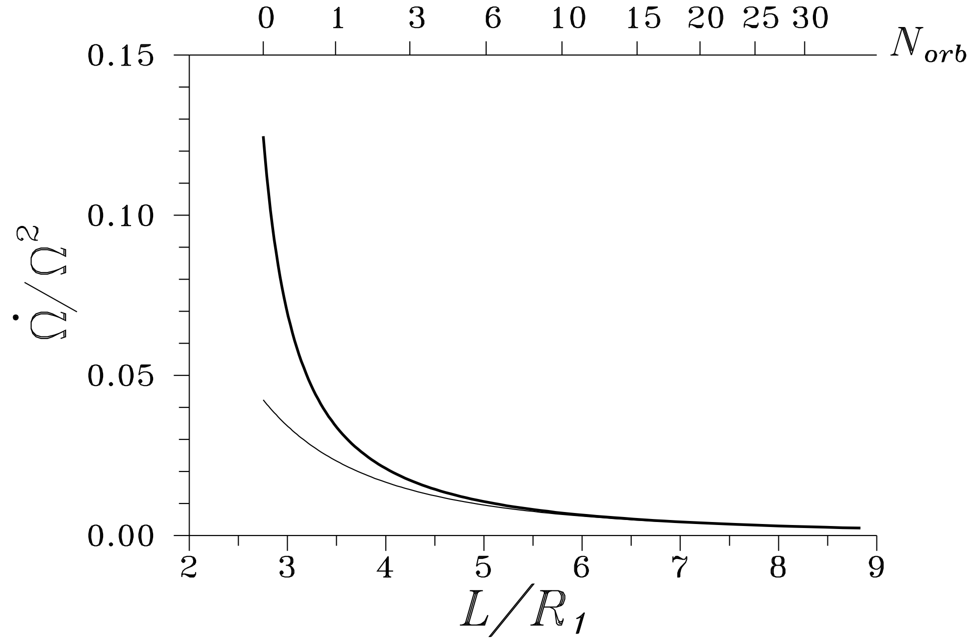

Figure 6: *Ratio of angular and centrifugal accelerations as a function of the distance between components for the cases of extended masses (thick line) and point masses (thin line).*

case of extended masses yields a higher velocity: at the end of convergence, this velocity is $0.016c$ for the case of extended masses and $0.005c$ for the point-mass case. Note also that the convergence velocity at the moment of contact would increase to $0.114c$ if we did not take into account both the mass distribution and the 'geometrical' distribution of the components; i.e., if we assumed that stars remain spheres with a fixed radius R_1.

Figure 5 presents the characteristic convergence time of the components $\tau = L/\overset{\bullet}{L}$ in units of orbital period P_{orb} as a function of the distance between the components. The dashed line corresponds to the characteristic hydrodynamic time, which indicates the rate at which equilibrium is reached inside a star. We can see from this plot that the star as a whole is nearly in hydrodynamic equilibrium right up to the moment of contact.

A comparison of the angular acceleration $\overset{\bullet}{\Omega}\ L$ and centrifugal acceleration $\Omega^2 L$ of the system is presented in Fig. 6 in the form of the ratio of these two quantities. This figure indicates the errors in our estimates of the power of the gravitational-wave radiation, which were obtained assuming that the components move along circular orbits at constant speed.

Figures 7–9 depict the solution of the resulting differential equation for L in the form of the functions $L(t)$, $\nu_{gw}(t)$ ($\nu_{gw} = 2\Omega/(2\pi)$) and $\nu_{gw}^{-8/3}(t)$. This last relation is interesting in that it should be linear in the case of point-mass binary,

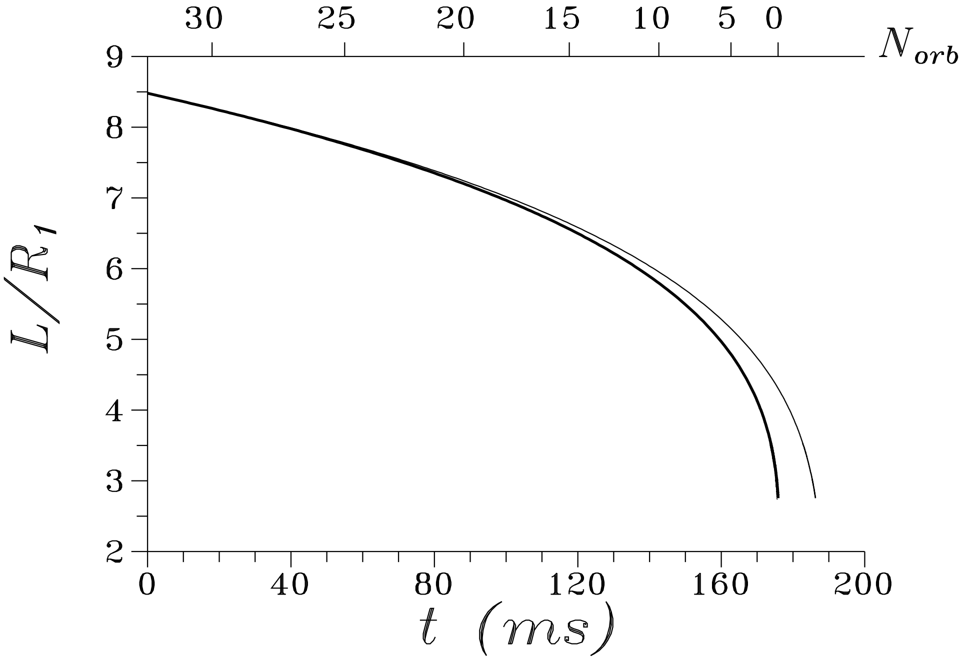

Figure 7: *Time dependence of the semi-major axis $L(t)$ for model with extended masses (thick line) and point masses (thin line).*

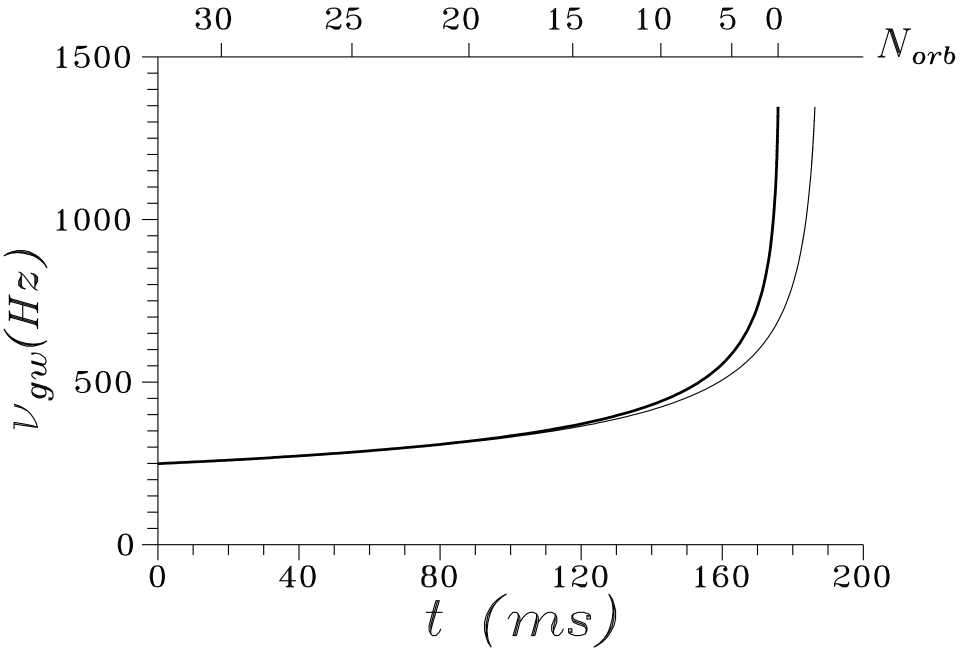

Figure 8: *Time dependence of the frequency of gravitational waves (in Hz) for models with extended masses (thick line) and point masses (thin line).*

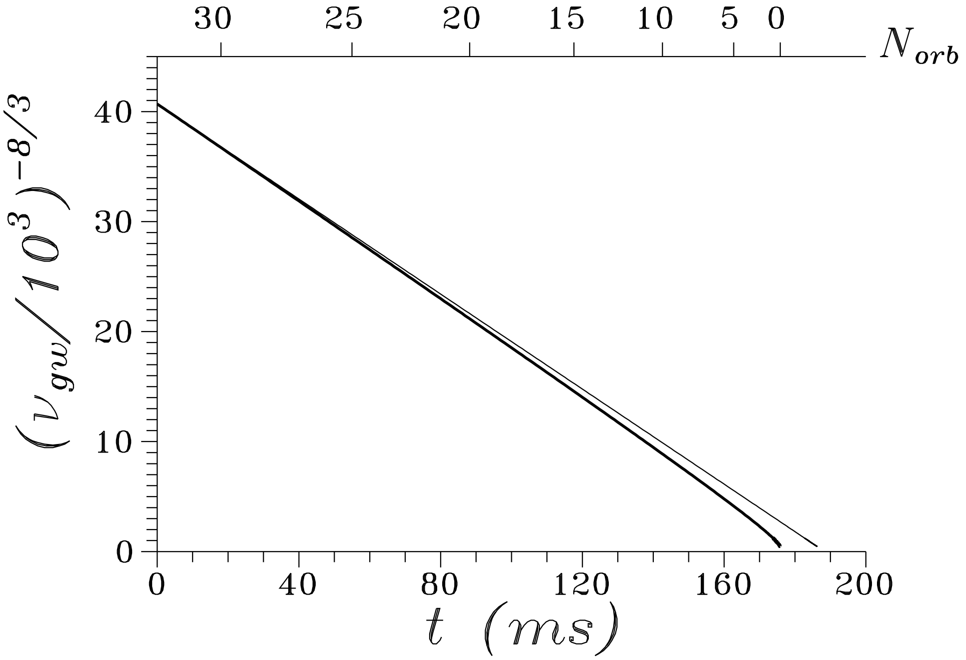

Figure 9: *Linear gravitational-wave frequency to the $-{}^{8}/_{3}$ power for models with extended masses (thick line) and point masses (thin line). This quantity is a linear function of time in the point-mass case.*

since $\dot{L} \sim L^{-3}$; $L^4 \sim t_0 - t$; $\nu_{gw} \sim L^{-3/2}$).

The waveforms h_+^{TT} for the signals from two merging neutron stars are shown in Fig. 10. We can see that the stars in a binary with extended masses come into contact 10.5 ms earlier than in the point-mass model. The phase shift for these two cases at contact $\delta\mathcal{N} = 5.97$.

The time dependence of the correlation coefficient χ between the signals from the point-mass and distributed binary systems is shown in Fig. 11. This correlation coefficient is determined by the formula

$$\chi(t) = \int_0^t h_1 h_2\, dt \Bigg/ \left(\int_0^t h_1^2\, dt \int_0^t h_2^2\, dt \right)^{1/2} ,$$

where h_1 and h_2 are the signals from the extended-mass and point-mass systems, respectively. The correlation is disrupted 70 ms before contact.

Figure 12 shows the binary system configurations (a) at the beginning of the calculation ($t = 0$, $L = 85$ km) and (b) at the time when the Roche lobes of the components are filled (contact). The time interval between these configurations id 17.8 ms, which corresponds to 32 revolutions of the system.

Note that the Jeans criterion for the dynamic stability of the system [10]

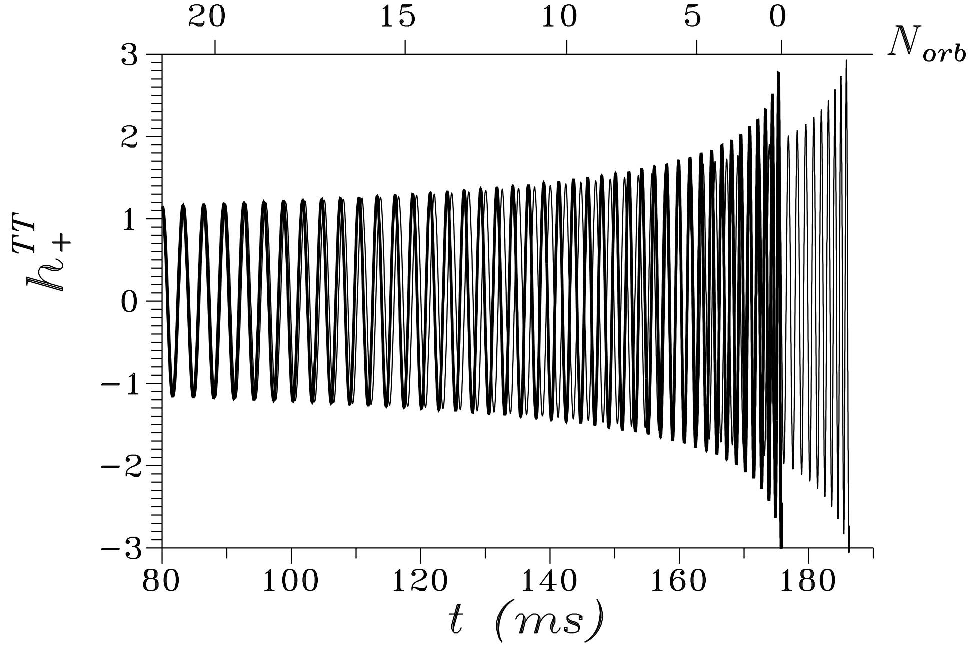

Figure 10: *Wave forms* h_+^{TT} *for the signals from two merging neutron stars. We can see that a binary system with extended masses (thick line) reaches contact 10.5 ms earlier than the point-mass system (thin line). The phase shift at the time of contact is* $\delta\mathcal{N} = 5.97$.

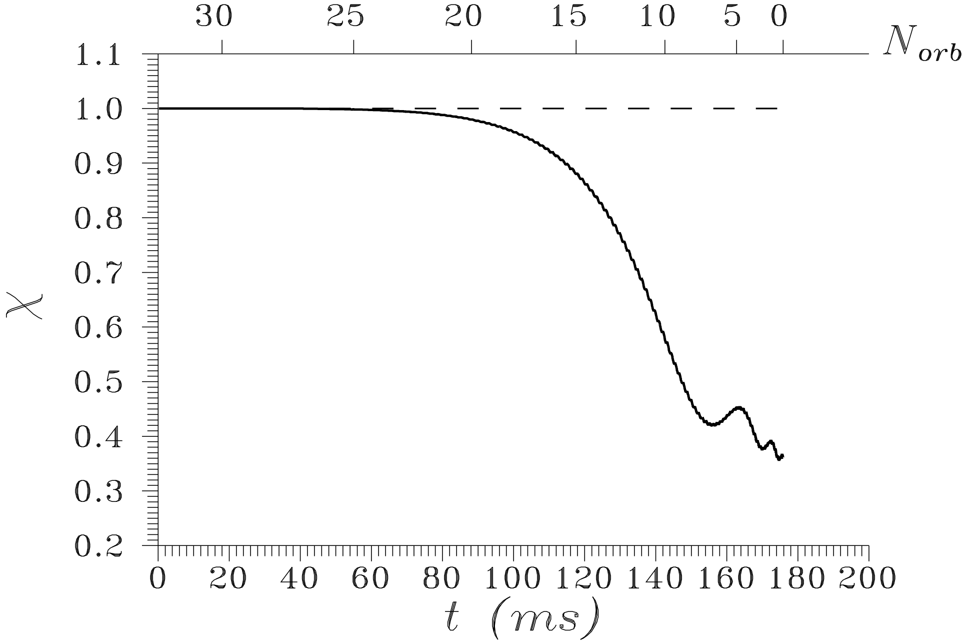

Figure 11: *Time dependence of the correlation coefficients of the signals from extended-mass and point-mass systems.*

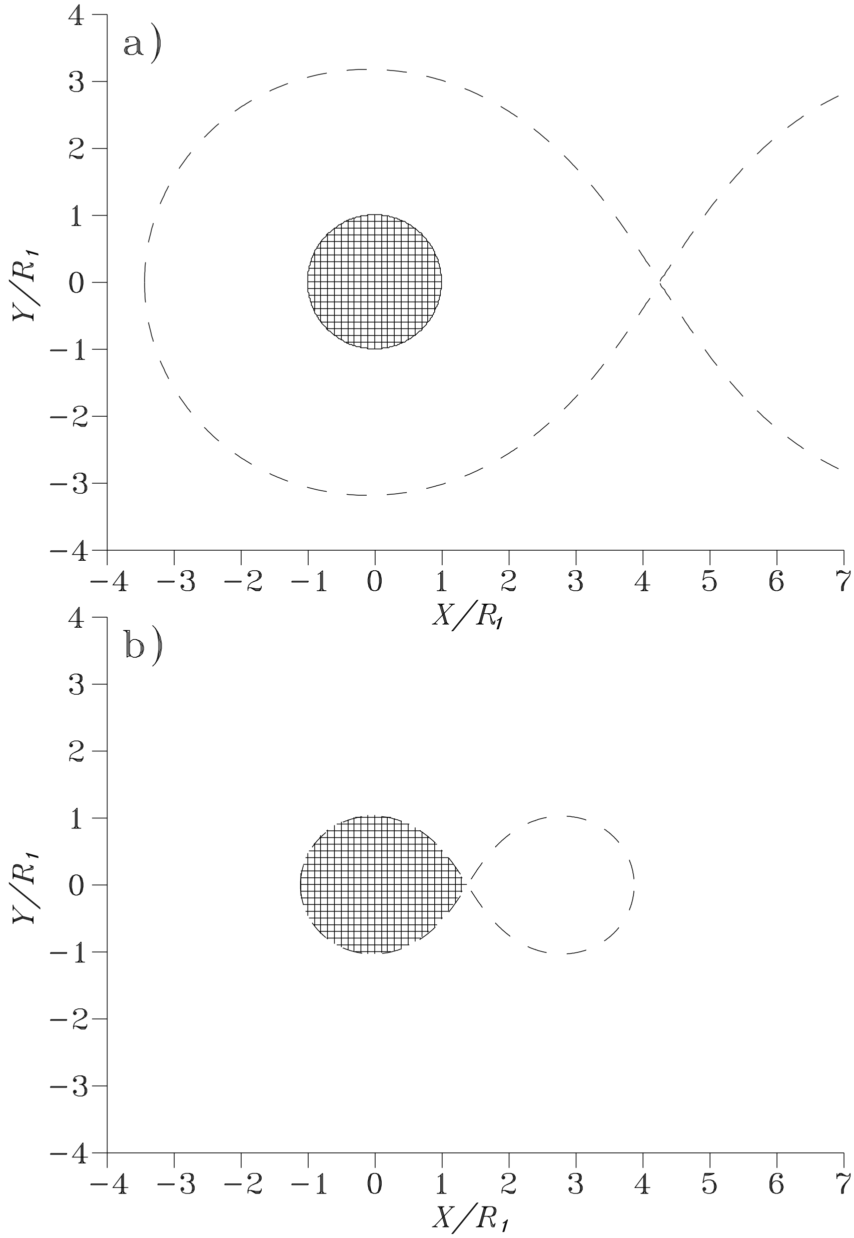

Figure 12: *Binary system configurations (a) at the beginning of the calculation ($t = 0$, $L = 85$ km) and (b) at the time when the Roche lobes of the components are filled (contact). The time interval between these configurations id 17.8 ms, which corresponds to 32 revolutions of the system.*

$$J_{rot} < {}^1\!/_3 J_{orb} \, ,$$

remains undisrupted right up to the time of contact (J_{rot} is the axial angular momentum of the components, and J_{orb} is their orbital angular momentum).

8 CONCLUSION

After gravitational-wave detectors begin to operate, the first date on the frequency and characteristics of merging binary neutron stars will become available. The gravitational-wave signals from such events will be detected by convolving a known waveform (the calculated signal from two neutron stars in a point-mass model, for example) with the output of the gravitational-wave detector. The output of the gravitational-wave detector can be represented in the form

$$s(t) = A \cdot S(t) + n(t) \, ,$$

where $S(t)$ is a given waveform with unknown amplitude and $n(t)$ is detector noise. The search for a signal using a least-square method or other suitable technique reduces to finding the minimum of a functional with respect to the unknown parameter A, the signal amplitude. This procedure can be rewritten in terms of integrals of the form $\int_0^t S^2(t)\, dt$, and so forth.

However, if the convolution is performed using a signal of the wrong form (in our case, the signal corresponding to two point masses) the effective signal will be diminished. This may result in false estimates of the signal level. Figure 11 shows the convolution of the signal corresponding to our model with that for a pair of two point masses. We can see that the convolution with the standard waveform leads to the rapid decrease of the registered signal ~ 70 ms before contact. Note also that the region over which $\alpha(L)$ differs appreciably from unity falls into the frequency band for the peak sensitivity of planned gravitational-wave detectors [18]. Therefore, it is important to take into account the distortion of the waveform when attempting to register a gravitational-wave signal.

It is evident that the distortions of the waveforms of gravitational-wave signals will impede detection of gravitational-wave events. On the other hand, precisely these distortions may prove to be very important for studies of the internal structure and equation of state of neutron stars.

ACKNOWLEDGMENTS

The authors thank N.I.Shakura, K.A.Postnov, and S.B.Popov for useful discussions. This work was partially supported by Russian Foundation for Basic Research (project no. 97-02-16486).

REFERENCES

1. Phinney, E.S. 1991, ApJ, 380, L17
2. Narayan, R., Piran, T., & Shemi, A. 1991, ApJ, 379, L17
3. Schutz, B.F. 1986, Nature, 323, 310
4. Lipunov, V.M., Nazin, S.N., Panchenko, I.E., Postnov, K.A., & Prokhorov, M.E. 1995, A&A, 298, 677
5. Thorne, K.S. 1987, in *Three Hundreds Years of Gravitation*, eds. S.W.Hawking, W.Israel, Cambrige Univ. Press, Cambridge, NY, p.330
6. Abramovici, A., et al. 1992, Science, 256, 325
7. Lincoln, C.W., & Will, C.M. 1990, Phys.Rev.D, 42, 1123
8. Blanchet, L., Damour, T., & Iyer, B. 1995, Phys. Rev. Lett., 74, 3515
9. Zakharov, A.V. 1996, Astron. Reports, 40, 552
10. Lai, D., Rasio, F.A., & Shapiro, S.L. 1993, ApJ, 406, L63
11. Ruffert, M., Rampp, M., & Janka, H.-Th. 1997, A&A, 321, 991
12. Kuznetsov, O.A. 1995, Astron. Reports, 39, 450
13. Landau, L.D., & Lifshitz, E.M. 1975, *The classical theory of fields*, Pergamon, Oxford
14. Chandrasekhar, S. 1939, *Introduction to the study of stellar structure*, Univ. Chicago Press, Chicago
15. Zel'dovich, Ya.B., & Novikov, I.D. 1967, *Relativistic Astrophysics*, Nauka, Moscow (in Russian)
16. Landau, L.D., & Lifshitz, E.M. 1980, *Statistical physics. Part I*, Pergamon, Oxford
17. Brown, G.E., Weingartner, J.C., & Wijers, R. 1996, ApJ, 463, 297
18. Thorne, K.S. 1993, in *Particle Astrophysics*, eds. G.Fontaine, J.Trân Thanh Vân, Editions Frontieres, Gif-sur-Yvette, p.375